

# Transmission performance analysis of 5.76 Tbps MC-WDM system incorporating optical wireless communication

YOUSIF I. HAMMADI<sup>1,\*</sup>, OMAR ABDULKAREEM MAHMOOD<sup>2</sup>

<sup>1</sup>*Bilad Alrafidain University College, Diyala, Iraq*

<sup>2</sup>*Department of Communications Engineering, College of Engineering, University of Diyala, Iraq*

This paper details a really high-speedness optical wireless communication (OWC) approach that integrates wavelength-division-multiplexing (WDM) capabilities and is based on the multi-carrier generation (MCG) idea. A novel approach for designing broad and flattened spectrum MCG is presented leading to 64 spectral lines source using a single continuous wave (CW) laser. With the help of this MCG, using a unique laser source to service many subscribers, the WDM networks wireless platform is extremely expensive, reliable, and delivering wide throughput for triple play applications to a large number of customers, with a total capacity of 5.76 Tbps. The impact of changing the refractive index architectural factor of the optical wireless model from  $5 \times 10^{-16}$  to  $5 \times 10^{-12} m^{-2/3}$  is investigated. The bit error rate (BER), optical signal to noise ratio (OSNR), and eye diagrams of the whole system were calculated in order to evaluate the functionality. In furthermore, the comprehensive power budget is reviewed in order to ensure that the findings are accurate.

(Received November 28, 2021; accepted April 7, 2022)

*Keywords:* OWC, MCG, MC-WDM, Photonic filter, Refractive index structure parameter, Spectral ripple

## 1. Introduction

Advancements in telecommunications engineering have put new capacities of downlink and uplink operations. Accordingly, subscribers became more satisfied with these improvements. In past decades, only free-space wireless telecommunications are capable to support communicating operations. However, the advancements in wireless communication systems made the optical wireless systems applicable as well.

Along with its adaptability and portability, optical wireless communication (OWC) systems are extensively utilized nowadays. In part as a result of these features, the range of applicants that can be incorporated and implemented through into (OWC) systems have grown considerably. Many implementations, including as multimedia, real-time programs, supervision systems, and other software applications, are now available for use over wireless networks [1-4]. Power management for wireless networks is a significant problem in today's society. This is because the vast majority of wireless gadgets are battery-powered. Battery performance may be extended with solid power control [5]. When compared to optical fiber, OWC uses the very matching principle and it has the same capabilities as optical fiber, but the optical light passes through the atmosphere rather than the heart of the optical system, which allows for the removal of the generating optical fiber and time [6, 7]. There are many benefits to using this technique, including the fact that it is impervious to radio frequency interference, offers fast data rates at little power, is very secure, and is inexpensive. For WDM systems, the data rate carried by each wavelength channel has grown massively to meet the ever-increasing capacity require-

ment in optical networks. Networks with connection speeds of 100 GB/s per line have been marketed since the middle of 2010 [8], while transmission rate of 200 GB/s per line have just been verified. Experiments have shown optical transmission with per-channel data rates exceeding 100 Gb/s and up to several Terabits/s (Tb/s), thanks to the advent of optical super-channels, which circumvent the electrical bottleneck via optical parallelism [9, 10].

In later years, the premise of a super-channel was broadened to include any collection of optical signals which are modulated and combined together along with spectral efficiency (SE) around the same initiating site, broadcasted and relayed together over that optical link, and then received at the same destination site [11-13]. MC-WDM has been proposed as a potential alternative to Nyquist-WDM, quasi-Nyquist-WDM, and orthogonal frequency division multiplexing in order to obtain high-SE multiplexing. Presently, the confluence of optical and wireless networks seems to have become a difficult study topic for improving Quality-of-Service (QoS) and increasing data transmission capacity to accommodate multimedia services [14-16].

Triple play operations need optical MC Generation (MCG) flexibility at the optical transmission side during the next optical network infrastructure because of the exponential development of packet activities. Many benefits come from utilizing MCG in this kind of system, including decreased system size, economic viability of optoelectronic devices or tunability lasers, and entertainment for a huge number of participants through backhaul data transfers in communication networks. The traditional way to offer these configurations in a WDM system used to be to uti-

lize several laser supplies or a single strong tune-able laser generator [17-19].

When there are a large number of customers, the broadcaster becomes larger because more lasers are needed. High power operations, maintenance, and increasing costs are all significant concerns. Since a result, putting an MCG source on the transmitter side looks like a good idea, as it will enable subscribers more room to transfer multimedia content while using less power and spending less money [20]. As a result, we developed a network connectivity founded on multi - carrier WDM.

Ultimately, the aim of this research is to investigate the design and operation of  $64 \times 90$  Gbps (5.76 Tbps) WDM networks systems based on the MCG paradigm. Each wavelength transmits at a transmission rate of 90 Gbps using optical intensity modulation format with a repetition rate of 30 GHz between sub-channels to achieve spectral efficiency of 3 bits per second per Hz (b/s/Hz). The analysis is carried out for  $64 \times 90$  Gb/s (5.76 Tbs) PSK WDM optical wireless system at transmission reach from 50 km to 500 km. Once the acquired bit error rate (BER) exceeds the BER criterion, the longest transfer lengths are logged. The following new features of this work are claimed as a result of the debate that has gone before it. The 90 Gbps data transmission rate is achieved utilizing a very stable MCG with small spacing, accomplished with a single CW laser. To that same authors' knowledge, this will be the first instance a 5.76 Tbps MC-WDM-based OWC has been made available. The suggested MC-WDM design, which is both dependable and cost-effective, offers the best option for meeting the bulk of 5G and beyond needs.

## 2. Design of multi-carrier generation

This section introduces the proposed multi-carrier generation (MCG) configuration with analytical model to describe its operation and characteristics. Nonlinear phase and intensity modulation via a succession of optical modulators generates MCG with ultra-dense spacing. In order to operate, the MCG requires just a single CW laser source, a single optical phase modulator (OPM) followed by optical electro-absorption (OEA) modulator, polarization controller (PC), and a phase shifter (PS), as illustrated in Fig. 1. The optical modulators modulate the CW Laser (CWL) with the microwave signal (MS). We modify the DC voltage level and the MS magnitude to get a vast group of optical subcarriers from the MCG's output, which we then analyze.

The mathematical methodology may be used to derive the mathematical framework characterizing the suggested MCG's output:

$$U_{out}(t)_{MCG} = T_{OPM}(t) \times T_{OEA}(V) \quad (1)$$

where  $T_{OPM}(t)$  and  $T_{OEA}(V)$  is the transfer function of the OPM and OEA, respectively.  $T_{OPM}(t)$  can be expressed as:

$$T_{OPM}(t) = \sum_{m=-\infty}^{\infty} J_m(n_1) \times e^{jmws_t} \quad (2)$$

Here,  $w_s = 2\pi v_s$ , and  $v_s$  is the repetition rate of the microwave signal, and  $n_1$  is the modulation index of OPM. where  $J_m(\cdot)$  denotes the  $m^{\text{th}}$  order of the Bessel function of first kind. To verify the generation of multiple wavelengths, To illustrate, let us examine the light beam that is emitted by the CWL as described in the following:  $U_{LD}(t) = \sqrt{p_{LD}} \times e^{jw_{LD}t}$ , where  $U_{LD}(t)$  denotes the optical field related to CWL,  $p_{LD}$  and  $w_{LD} = 2\pi v_{LD}$  show the CWL's wattage and frequency., respectively. The CWL is modulated by the MS of a repetition rate of  $v_s$  at the first MCG, leading to generate of many wavelengths with the spacing equals to the repetition rate of the MS. OPM produces a modulated light beam at its output, which may be represented as follows:

$$U_{OPM}(t) = \sqrt{p_{LD}} \sum_{m=-\infty}^{\infty} J_m(n_1) \times e^{j(w_{LD}+mw_s)t} \quad (3)$$

The comparatively tiny signal approximation is utilized to assess the produced overtones and spectral bandwidth of the OEA, and the transfer function of the OEA is extended by utilizing a Taylor series around the Voltage level to get the transfer function of the OEA. Consider that the biasing voltage of the modulator is  $V_{dc}$ , at the same time, the output of the modulator is  $V_{ac}(t)$ , accordingly, the deriving voltage, which will be fed is the summation of these two voltages. Hence, the OEA function is:

$$T_{OEA}(V) = \sum_{-\infty}^{\infty} \frac{1}{x!} R_x [A_s \cos(w_s t)]^x \quad (4)$$

As a result, by substituting eqn. (4) into eqn. (1), the various wavelengths produced at the output of MCG may be derived as follows:

$$U_{out}(t)_{MCG} = T_{OPM}(t) \times \sum_{-\infty}^{\infty} \frac{1}{x!} R_x [A_s \cos(w_s t)]^x \quad (5)$$

It may be understood from eqn. (5) that, the center wavelength of the multiple wavelengths is determined by the center wavelength of the CW laser. The MCG can generate wavelengths in a wide frequency range of the electrical driving signal. Additionally, notice that all of the wavelengths are evenly spaced apart; this is a common observation. Further, they are positioned to frequencies  $v_m = v_{LD} + mv_s$ , where  $m = 0, \pm 1, \pm 2, \pm 3, \dots$ . With the aid of a photonic filter with the transfer function provided in eqn. (6), the various wavelengths produced at the end of MCG are blocked out, to select the flattened wavelengths within 1 dB spectral ripple,

$$H(v) = \begin{cases} \rho & v_c - 0.5B < v < v_c + 0.5B \\ d & \text{others} \end{cases} \quad (6)$$

Thus, in the last expression, the different parameters can be defined as follows:

- $\rho$  is the insertion loss,
- The depth denoted by  $d$ ,

- The center frequency of the filter is represented as  $\nu_c$ ,
- The bandwidth is given by  $B$ ,
- While  $\nu$  is the frequency.

Among the multiple wavelengths available at the output of the MCG, by using the photonic filter, we choose 64 wavelengths located at frequencies  $\nu_m = \nu_{LD} + m\nu_s$ , where  $m = 0, to 63$ , since these wavelengths have almost the same power level (i.e., within 1 dB spectra ripple). These filtered wavelengths are used as optical carriers to implement the advanced wavelength division multiplexing system, which is called MC-WDM system. The simulation parameters of the MCG are listed in Table 1, as will be explained in the next section.

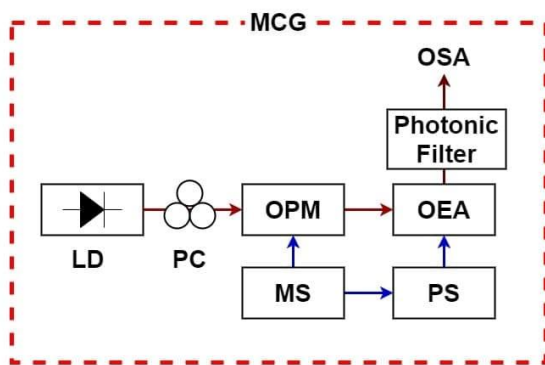


Fig. 1. Configuration of the MCG

### 3. Configuration of MC-WDM Optical Wireless System

The evaluation of the proposed solution, which incorporates the suggested optical MCG, is examined in this section. It is utilized as the fundamental WDM optical generator, with sixty-four spectral lines (corresponding to a 1 dB-flatness area) and 30 GHz channel separation being manipulated by a 90 Gbps PSK signal per connection on a single MCG. As shown in Fig. 2, the three subtopics under consideration in the MC-WDM optical wireless communication technologies under study are the transmitter, optical wireless (OW) channel, and receiver (all of which are represented by block diagrams).

Consider the first topic, which is the transmitter, is comprises of MCG, wavelength selective switch (WSS), optical modulators, and optical combiner. A 1 by 64 WSS is used to screen out the wavelengths of interest. In order to generate 64 intensity modulated optical signals, each outputted wavelength of the WSS is fed into an intensity modulator (IM), which is then intensity modulated by the PSK baseline data at a rate of 90 Gbps to produce 64 intensity modulated beam. The resultant outputs are sent into a 64-by-1 optical combiner with a width of 15 GHz, with the type and order of component filters being Bessel and 2,

respectively, while the capacity of the combiner is 15 GHz. These intensity optical signals are combined to deliver an optical WDM signal to an OW channel. The transmission link consists of OW channel followed by an optical erbium doped fiber amplifier (EDFA.) to compensate power losses. The OW connection used in this study is comprised of two radiator components that are spaced apart from one another and from the transmission channel by a predetermined distance. Because of the dense packing of optical channels, it is necessary to adjust the gain of the optical amplifier in place to evade the production of four wave mixing-based crosstalk. A sufficient amount of signal amplification is achieved using an optical amplifier, and the amplified signal is then delivered straight to the recipient side for treatment. 1:64 demultiplexer is used to divide the acquired MC-WDM signal at the receiver end of the transmission path and optically filtered by Gaussian filters to ride over channel specific wavelength. Thus, each received channel is treated independently. Because it has superior performance features than the positive intrinsic negative (PIN) photodiode, the avalanche photodiode (APD) is employed for the detection purposes on the output side of the system. APD is capable of measuring even low-level light and, as a result of its high sensitivity, fast response time, and internal gain mechanism, it is extensively employed in optical measuring distances and optical communications with long-distance transmissions, among other applications. The data from each demultiplexed stream is then retrieved using a low pass filter (LPF) and a PSK demodulator, which are both implemented in software.

The transmitter, channel, and receiver sides of the simulated system have all been setup for a particular set of conditions on the transmitter side. According to the needs of the system model, the parameters are chosen whether on the account of their kind or on the account of their theoretical value. A summary of the planned MC-WDM system parameters may be found in Table 1. To evaluate the performance of MC-WDM optical wireless communication system, it is necessary to use optical power meters (OPMs), optical spectrum analyzers (OSAs), and BER quantitative measurements. OSAs, on the other hand, offer the capability of analyzing the optical spectrum. OPM is a unit of measurement for the power supplied in decibels (dBm). The BER analyzer determines the BER value and shows an eye diagram in real time without the need for human intervention. The bit error rate (BER) is often a standard data value provided by any transmission systems. The bit error rate (BER) is the number of error detection received calculated by dividing the number of bits sent across the transmission medium. The majority of the time, these bit mistakes are caused by noise or other entanglements.

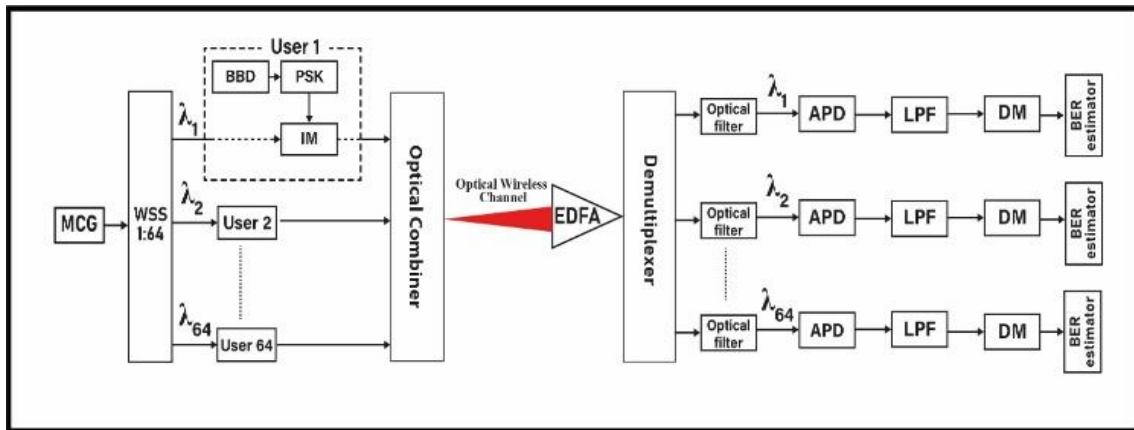


Fig. 2. Schematic Diagram of MC-WDM optical wireless system

Table 1. Simulation Parameters for MC-WDM Optical Wireless System

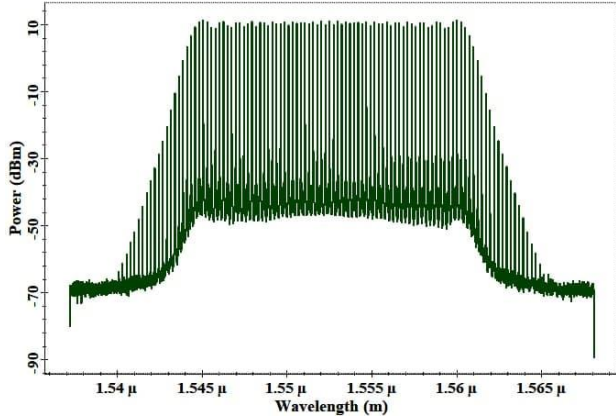
Component	Parameter	Value
<b>System layout</b>	Bit rate (Gbps)	90
	Sequence length (bits)	512
	Samples per bit	64
	Number of samples	8192
<b>MZM</b>	Extinction ratio (dB)	25
<b>OWC channel</b>	Wavelength (nm)	1552.5
	Transmitter aperture diameter (cm)	5
	Receiver aperture diameter (cm)	20
	Transmitter optics efficiency	0.8
<b>APD photodiode</b>	Receiver optics efficiency	0.8
	Beam divergence (mrad)	1.5
	Responsivity (A/W)	0.9
	Dark current (nA)	5
<b>LPF</b>	Thermal power density (W/Hz)	$1 \times 10^{-24}$
	Cutoff frequency	$0.75 \times \text{Bit rate}$
<b>Laser diode</b>	Center wavelength (nm)	1552.5
	Power (dB)	10
	Linewidth (MHz)	100
<b>Microwave signal</b>	Repetition rate (GHz)	30
<b>OPM</b>	Phase deviation (degree)	90
	$V_{\pi}$ Voltage (volt)	3
<b>OEA</b>	Generated Bandwidth (THz)	3.84
<b>Photonic filter</b>	Order	3
	Roll Off factor	0.5
	Bandwidth (THz)	1.92

#### 4. Results and discussion

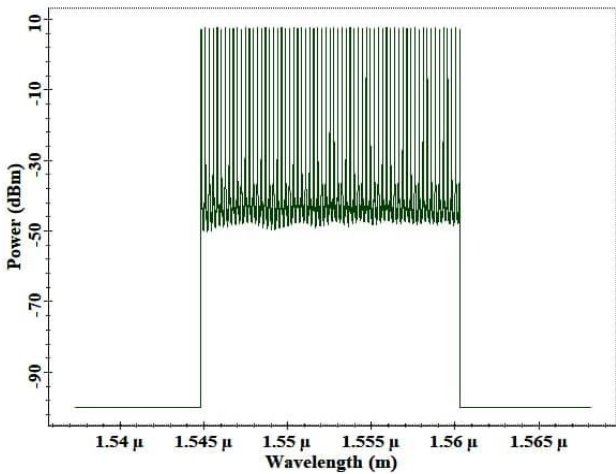
To explore the gain of using the proposed optical MCG, the performance of MC-WDM implementing of the MCG as a WDM source is investigated in this section. Next, the simulation results of the MC-WDM system that carried out by VPItransmissionMaker® commercial

software are demonstrated. The simulation results are evaluated based on the system that described in Section 3. The MCG is powered by a laser source with a wavelength of 1552.5 nm and is intended to have line spacing of 30 GHz. MCG's optical spectrum, as shown in Fig. 3a, is made up of 127 different wavelengths that are all interconnected. Where 64 wavelengths of them within

1dB-spectral ripple are selected using the photonic filter as illustrates in Fig. 3b. Using the designed MCG, a total bandwidth of 3.81 THz may be produced. Whereas the bandwidth of flatened lines is 1.91 THz.



(a)

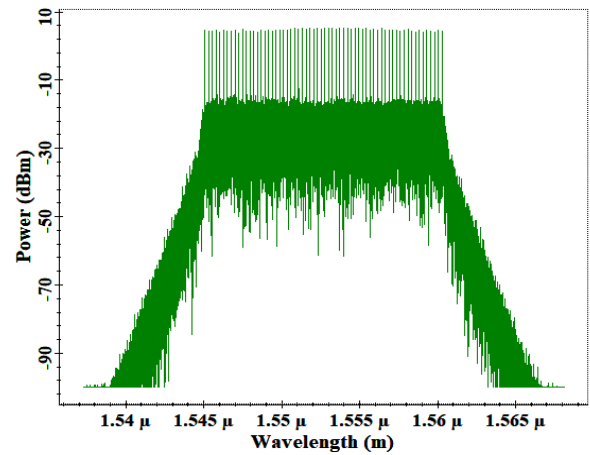


(b)

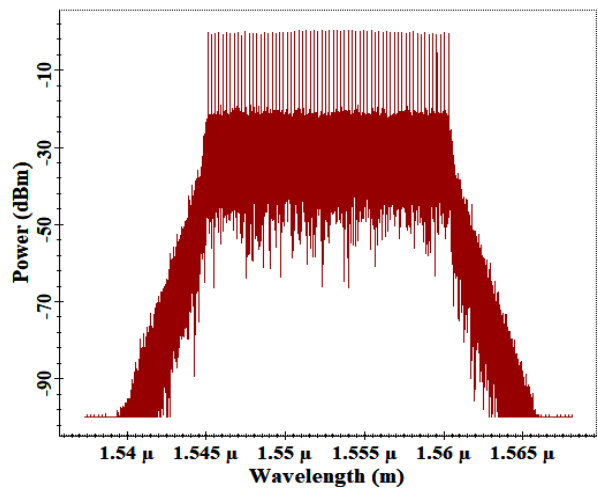
Fig. 3. Spectrum of Optical Multi-carriers: (a) Output of the MCG, (b) Output of the photonic filter

MC-WDM optical sources such as the MCG are utilized as the foundation of the system, with sixty-four wavelengths, which stands for 1 dB spectral ripple area, and 30 GHz channel gap being modulated by a 90 Gbps PSK signal each connection. The block diagram in Fig. 2 depicts the three subtopics of the MC-WDM optical network under study, in a simplified manner. Presented in this part are the simulation outcomes of 64-by-90 GSymbol per second PSK delivery, with all of these channels operating at a data rate of 90 Gbps. The overall data rate of the superchannel is 64 times 90 Gbps, which is equivalent to 5.76 Tbps. The symbol rate can be determined following the formulae  $R_s = R_b / \log_2 M$ , in which,  $M$  stands for the symbols quantity. Hence, each individual-line bit rate determined to be 90 Gbps. Worth mention that  $M = 2^i$ , where the count of bits in each symbol is denoted by  $i$ . For instance, suppose that the 8-

PSK format, in other words,  $M = 8$  ( $i = 3$ ), the symbol rate can be evidently found to be 30 Gsymbol/s. If we denote the roll-off factor for the filter, in this study the well-known raised-cosine was utilized, the modulated bandwidth can be formulated as  $BW = R_s + R_s \gamma$ . Consequently talking, the spacing of the utilized channel should be higher in value than the operating bandwidth. This setting will provide more room to avoid the phynomina known as crosstalk of adjacent channels That is, the bandwidth, using  $BW = R_s + R_s \gamma$  must be less than 30 GHz. After transporting across a distance of 70 kilometers in clear weather, the optical spectra of transmitting 64 wavelengths are shown in Fig. 4. The power has been found to be 6 dBm before and 5 dBm after the 70-kilometer range via a weak-turbulence zone. The individual sub-channels are communicates at 90 Gbps, with frequency spacing of 30 GHz, resulting in a SE of 3 b/s/Hz.



(a)



(b)

Fig. 4. Optical spectra of the WDM signal (a) Output of the MC-WDM transmitter (b) Output of the optical wireless channel

According to the power allocation of an optical network, it is possible for the developer to guarantee that the system will perform as intended in terms of reliability, such as system span, total number of consumers, compatibility for data transmission, and so on. Because of this, a power cost evaluation is done out in order to determine the overall power outage throughout the planned infrastructure. It is necessary to calculate the total optical power outage,  $P_{Loss}$ , or the power of the received data before the detector in order to do the assessment. Achieving a  $P_{Loss}$  smaller than or equal to  $S_{rx}$  is critical for the system's performance, with  $S_{rx}$  representing the detection sensitivity being the most important factor.  $P_{Loss}$  may be computed using the prototype implementation shown in Fig. 2 by computing the power drop throughout various parts of the system. Thus,  $P_{Loss}$  may be expressed as follows:

$$P_{Loss} = P_{MCG} + P_{tx} + P_{link} + P_{rx} \quad (7)$$

$P_{MCG}$  denotes the power of the transmitted fibre departing the MCG, while,  $P_{tx}$  denotes the power of the transmitted fibre left the transmitter, which may be calculated by summing the power drops at the WSS,  $P_{WSS}$ , and the optical combiner,  $P_{Combiner}$ . As a result, the total transmit power exiting the emitter may be expressed as  $P_{tx} = P_{WSS} + P_{Combiner}$ . The dropping power of the signal over a communication path is calculated as the product of the length of the OWC ( $L_{OW}$ ) multiplied by the attenuation of the OWC plus the gain, which is due to the optical amplifier ( $P_{Amp}$ ). According to this,  $P_{link} = L_{OW} \times \alpha + P_{EDFA}$ . may be used to represent the entire signal power exiting the transmission link. Losses at the demultiplexer ( $P_{demux}$ ) and optical filters ( $P_{OF}$ ) together determine the power drop across the receiver. As a result,  $P_{rx} = P_{demux} + P_{OF}$ . may be used to express the receiver's overall power loss. Table 2 shows component information and insertion losses that are important. The overall power loss throughout the new methodology may be expressed as follows, using the information provided above as guidance:

$$P_{Loss} = P_{MCG} - P_{WSS} - P_{Combiner} - L_{OW} \times \alpha + P_{EDFA} - P_{demux} - P_{OF}. \quad (8)$$

$P_{Loss} = -3.1 \text{ dB}$  has been calculated using the information in the preceding study and in Table 2. APD detector minimal power levels can readily sustain the specified amount of customers, thus this system can easily support them.

Table 2. Description of the suggested system's power losses and gains

Component	Loss or Gain
MCG power	10 dB
WSS	2 dB
Combiner	2 dB
OW attenuation ( $\alpha$ )	0.43 dB/km
Optical amplifier gain	25 dB
Demultiplexer	2 dB
Optical filter	2 dB

BER against OSNR plots were used to examine the proposed MC-WDM system's OWC-BER performance. For the OWC, a random wavelength of 1552.5 nm was chosen at random for performance testing at various turbulence levels. Different BER values are produced by altering the signal OSNR after in-band optical noise has been introduced to the chosen channel. Fig. 5 depicts the relationship between BER and OSNR for various OWC attenuation levels. As low as the photodetector can accept optical power without generating a BER score of  $10^{-9}$  (which denotes the threshold of the BER), the receiver is said to be sensitive. Clearly shown in Fig. 5 that  $10^{-9}$  is reached when the OSNR reached 13 dB, 11 dB, and 10 dB for weak, moderate, and strong turbulence regime, respectively. According to Fig. 5, the OSNR decreases from mild to high turbulence environments when the amount of the  $C_2^n$  factor is increased. Even yet, the total BER performance of the received optical signal is extremely excellent, demonstrating the robustness of the transmission connection as well. In addition, the 1552.5 nm receiver constellation diagrams for mild, moderate, and severe turbulence regimes are shown highlighted in Fig. 5.

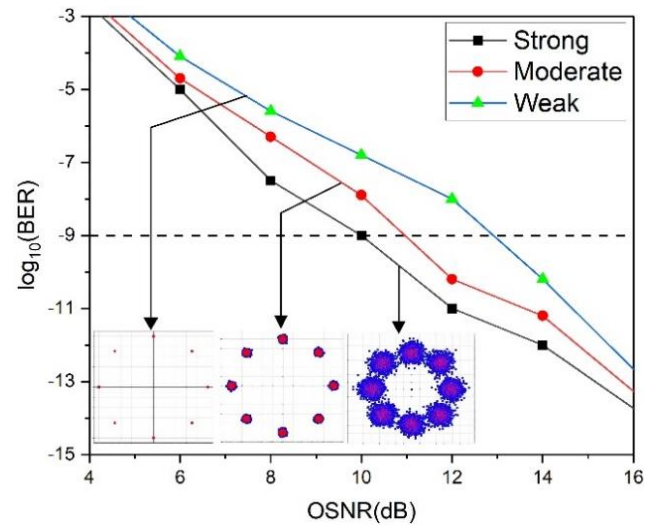


Fig. 5. BER versus OSNR at different turbulence regimes (color online)

So far, the eye-diagram, which is more investigates the system's performance, has not been illustrated, thus, as illustrated in Fig. 6, we go into more detail about the recommended platform's effectiveness using eye diagrams generated at a BER of  $10^{-9}$  for the chosen channel under various turbulence situations. DM produces eye diagrams as a byproduct. Fig. 6 shows that the OWC-based connection causes greater fluctuations in intensity on those caused by severe turbulence. There are no wide-open eye diagrams for turbulence situations because the variations in timing and amplitude from bit to bit make it difficult to distinguish between ones and zeros. Furthermore, there is an open eye for any situation that indicates a potential for success.

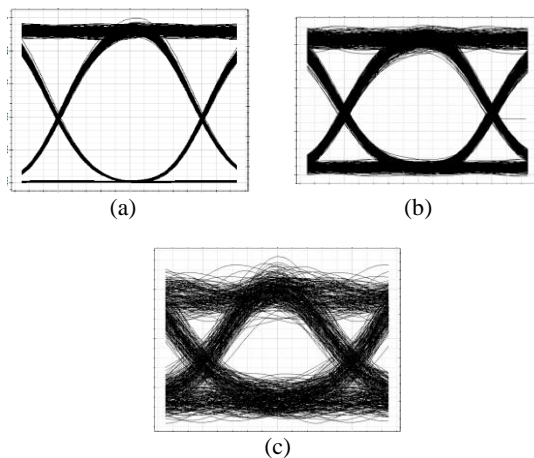


Fig. 6. Received eye diagrams of channel (1552.5 nm) at different turbulence regimes (a) weak (b) moderate (c) strong

## 5. Conclusion

A cost efficient and reliable optical wireless communication system  $64 \times 90$  Gbps MC-WDM architecture is proposed employing optical multi-carrier generation technique to support high spectral efficiency transmission system with large capacity of data transported. The data of 64 channels coded in PSK format are sent across a 500 km connection using 64 wavelengths produced from a single laser source with a 1dB-spectral ripple and a 30 GHz separation to enable the transfer of 5.76 Tbps data rate, resulting in a 3 b/s/Hz SE. The suggested platform's performance is assessed under various turbulence environments. OWC refractive index construction factor  $5 \times 10^{-16}$  to  $5 \times 10^{-12} m^{-2/3}$  is varied to see what impact it has. It has been shown that the OSNR value of around 13 dB, 11 dB, and 10 dB for weak, moderate, and strong turbulence regime, respectively at the threshold BER value. Additionally, the power budgeting of the designed system is investigated, as a result, it has no problem supporting the specified number of subscribers with APD detector nominal power ratings. The proposed MCG may also be modified and adjusted to provide 100 GHz line spacing and microwave photonic filters suited for arbitrary waveform creation and 5G mobile telecommunications development.

## References

- [1] Z. Ghassemlooy, S. Arnon, M. Uysal, Z. Xu, J. Cheng, IEEE Journal on Selected Areas in Communications **33**(9), 1738 (2015).
- [2] D. Tsonev, S. Videv, H. Haas, Optics Express **23**(2), 1627 (2015).
- [3] A. Boucouvalas, P. Chatzimisios, Z. Ghassemlooy, M. Uysal, K. Yiannopoulos, IEEE Communications Magazine **53**(3), 24 (2015).
- [4] D. K. Borah, A. C. Boucouvalas, C. C. Davis, S. Hranilovic, K. Yiannopoulos, EURASIP Journal on Wireless Communications and Networking **2012**(1), 1 (2012).
- [5] H.-Y. Wang, C.-H. Cheng, C.-T. Tsai, Y.-C. Chi, G.-R. Lin, Journal of Lightwave Technology **37**(13), 3388 (2019).
- [6] C.-H. Yeh, W.-P. Lin, C.-M. Luo, Y.-R. Xie, Y.-J. Chang, C.-W. Chow, IEEE Access **7**, 138927 (2019).
- [7] D. P. Agrawal, Q.-A. Zeng, Introduction to wireless and mobile systems, Cengage Learning, USA, 2015.
- [8] A. S. Gowda, A. R. Dhaini, L. G. Kazovsky, H. Yang, S. T. Abraha, A. Ng'oma, Journal of Lightwave Technology **32**(20), 3545 (2014).
- [9] C.-H. Yeh, J.-R. Chen, W.-Y. You, C.-W. Chow, IEEE Access **8**, 96449 (2020).
- [10] B. Corcoran, M. Tan, X. Xu, A. Boes, J. Wu, T. G. Nguyen, D. J. Moss, Nature Communications **11**(1), 1 (2020).
- [11] D. Novak, R. B. Waterhouse, A. Nirmalathas, C. Lim, P. A. Gamage, T. R. Clark, J. A. Nanzer, IEEE Journal of Quantum Electronics **52**(1), 1 (2015).
- [12] D. V. Coelho, P. Marciano, T. V. Coelho, M. Segatto, M. J. Pontes, Journal of Microwaves, Optoelectronics and Electromagnetic Applications **18**, 196 (2019).
- [13] P. Marin-Palomo, J. N. Kemal, T. J. Kippenberg, W. Freude, S. Randel, C. Koos, Optics Express **28**(9), 12897 (2020).
- [14] D. Sharma, Y. K. Prajapati, R. Tripathi, Photonic Network Communications **39**(2), 120 (2020).
- [15] M. Imran, P. M. Anandarajah, A. Kaszubowska-Anandarajah, N. Sambo, L. Potí, IEEE Communications Surveys & Tutorials **20**(1), 211 (2017).
- [16] L. N. Binh, "Advanced Digital: Optical Communications," ed: CRC Press, 2015.
- [17] S. Chandrasekhar, X. Liu, Systems and Networks **11**, 83 (2013).
- [18] S. Chaudhary, A. Sharma, N. Chaudhary, Journal of Optical Communications **37**(4), 375 (2016).
- [19] X. Chen, A. Al Amin, A. Li, W. Shieh, Optical Fiber Telecommunications VIB: Chapter 8. Multicarrier Optical Transmission, Elsevier Inc. Chapters, 2013.
- [20] L. Lundberg, M. Karlsson, A. Lorences-Riesgo, M. Mazur, J. Schröder, P. A. Andrekson, Applied Sciences **8**(5), 718 (2018).

\*Corresponding author: yousif.ibrahim.hammadi@gmail.com